

# Low Reynolds turbulence model CFD simulation for complex electronic system: an industrial point of view

**M.Giannuzzi**

Prompt Engineering srl - Via Livorno 60, 10144 Torino, IT

E-mail: [michele.giannuzzi@prompt-engineering.com](mailto:michele.giannuzzi@prompt-engineering.com)

**Abstract.** In electronic systems the presence of bluff bodies, sharp corners and bends are the cause of flow separation and large recirculation bubbles. Since the recirculation vortices develop they encapsulate the heat from an electronic component becoming one of the major contributors of malfunction. Going in depth in this, some numerical simulations of conjugate heat transfer for a heat wall-mounted cube have been performed using the commercial CFD code scSTREAM V11 by Software Cradle Co, Ltd. It is well known that the reliability of CFD analysis depends heavily on the turbulent model employed together with the wall functions implemented. The three low-Reynolds  $k-\varepsilon$  turbulent models developed by Abe-Nagano-Kondoh have been validated against experimental data consisting mainly of velocity profiles and surface temperature distributions provided in literature. The performed validation shows a satisfactory agreement between the measured and simulated data. The turbulent model chosen is then used for the CFD simulation of a complex electronic system.

## 1. Introduction

Nowadays the electronics industry sees a constant and ever more stringent technological progress. The adoption of new packaging and miniaturization processes increases the problems associated with the thermal load dissipation. Due to the presence of multi-property materials (such as printed circuit boards and integrated circuits), multiple heat sources and complicated internal geometries, the electronics systems are characterized by complex heat transfer behavior.

In [1] was addressed the importance of combining experimental and numerical approaches to understand the thermal behaviour of complex electronic devices. Testing campaigns were meant to give all the technical information necessary to reproduce a real system by means of numerical model. In this paper, time was spent analyzing hypotheses and guidelines modeling useful to simplify the virtual model maintaining high standard of result's reliability.

Under this framework when commercial numerical software is used, the unquestionable importance of a validation step for the numerical model is needed in order to assure the effectiveness and reliability of the results carried-out. Although CFD simulations are accepted as a design tool, they are still subject of modeling errors. It is well known that the reliability of CFD analysis depends heavily on the turbulent model employed together with the wall function implemented. In this communication, time was spent in choosing the most suitable turbulence model useful for electronic cooling simulation. To this aim, a virtual test campaign over a channel with a wall-mounted cube was performed. The turbulence models used in this study



have been validated with respect to the experimental data consisting mainly of velocity profiles and surface temperature distributions provided in literature [2; 3].

The commercial software scSTREAM V11 Thermo-fluid Analysis System by ©Software Cradle Co, Ltd, which is a structured/Cartesian mesh Finite Volume Method solver, has been used.

## 2. Which are the best turbulence models useful for electronic cooling simulation?

In electronic cooling systems off-design geometries such as bluff bodies, sharp corners and bends are mainly characterized by adverse pressure gradients for which the flow separates and large recirculation bubbles are generated [2]. Most electronics flows in the near-wall regions are characterized by strong viscous stress and wall blocking effects. Such separation and reattachment zones have a strong impact in temperature prediction profiles. By means of a literature overview, one can see that the high-Reynolds-number models are the most used in the field of electronic cooling simulations. However it is known that these models are unable to handle the near-wall region directly and they usually over-predict the heat transfer coefficient getting a lower surface temperature profile. From this, the need arises to exploit transitional and low-Reynolds number turbulent models. Moreover the importance of developing the technology to control turbulence and promote heat transfer is not a niche anymore, and in the last decades great effort on modeling near-wall turbulence has been spent. In this study, one of the latest low-Reynolds  $k - \varepsilon$  model is used, *i.e.* the one developed by Abe-Nagano-Kondoh (AKN) [4; 5]. In scSTREAM V11 [6] several turbulence models can be found such as the standard  $k - \varepsilon$ , the RNG  $k - \varepsilon$ , the MP  $k - \varepsilon$ , the linear low-Reynolds-number  $k - \varepsilon$ , the non-linear low-Reynolds-number  $k - \varepsilon$ , the temperature field two-equation models (in which the air properties are temperature dependent) and the Large Eddy Simulation models. Since the interest is for electronic cooling problems only low-Re number models have been considered.

### 2.1. Linear low-Reynolds Abe-Nagano-Kondoh model

In Iaccarino [7] a low-Re model with the Launder and Sharma damping function [8] has been used for solving a steady flow in asymmetric, two-dimensional diffuser. The numerical predictions are in poor agreement with the experimental data since the model fails to respond correctly to the adverse pressure gradient and misses the separation and the recirculation completely.

By contrast, the linear AKN model allows accurate analysis of a wide range of flows, with Reynolds numbers ranging from low to high. It is able to achieve a significant improvement on conventional turbulence models in terms of accuracy of prediction of separation and reattachment flows. Moreover it is also valid for the analysis of the transition from laminar to turbulent flow, or the reverse transition from turbulent to laminar flow. The basic equations used in this low-Reynolds-number turbulence model are basically the same of those used for high-Reynolds-number turbulence models. The strong viscous stresses and the damping effects of turbulence are considered by adding some numerical terms: the most important is the damping function  $f_\mu$ .

$$\mu_t = \rho C_\mu f_\mu \frac{k^2}{\varepsilon} \quad ; \quad f_\mu = \left(1 - e^{-\frac{y^+}{14}}\right)^2 \left[1 + \frac{5}{R_t^{3/4}} e^{-\left(\frac{R_t}{200}\right)^2}\right]$$

### 2.2. Non-linear low-Reynolds AKN model

In Klebanoff [9] has been demonstrated the importance of the region near the wall where the most turbulent energy is generated and the inadequacy of the concept of local isotropy. One of the limitations with Eddy Viscosity models is that they use an isotropic value which may not be appropriate and hence can increase the diffusion of the results obtained. This means that linear turbulence models are completely unsuited for the analysis of flow in which secondary

eddies arise. By contrast, the non-linear turbulence model can be applied to the phenomenon of anisotropic turbulence by deriving the coefficient of non-linear eddy viscosity from the spatial gradient of mean velocity. More information about the mathematics of this model can be found in [4; 6].

### 2.3. Two-equation heat transfer AKN model

The two-equation heat transfer AKN model (known as thermal AKN model) was proposed by Abe et al. [5]. It is based on the low-Reynolds-number AKN model but the prediction accuracy for the turbulent heat transfer coefficients is now improved. To get this, eddy diffusivity for heat  $\alpha_t = \frac{K_t}{\rho C_p}$  is represented by the temperature variance  $\bar{t}^2$  and its dissipation rate  $\varepsilon_t$  instead of a constant turbulent Prandtl number and the eddy viscosity. In [10] it is pointed out that the turbulent Prandtl number, which is widely used as a conventional approach to solve turbulent heat transfer problems, is not constant at all. In general, the turbulent Prandtl number strongly depends on the distance from walls. Furthermore, it is strongly influenced not only by a kind of fluid, but also by the existence of secondary flow, pressure gradient, buoyancy and even by thermal boundary conditions on heated surface. The assumption of the constant turbulent Prandtl number is valid till that both the velocity and the thermal boundary layers have the same thickness and are developing downstream in the same way. However, one cannot always expect to find this similarity in the turbulent flows. More information about the mathematics of this model can be found in [5; 6].

### 2.4. Analytical wall-function (AWF) for low-Reynolds number model

It is known that low-Reynolds-number turbulence model always requires strict no-slip boundary conditions. Indeed a strong clustering of the grid points at the walls should be used so that the  $y^+$  of the first grid point away from the wall is almost everywhere less than 1. However, it is quite difficult to assure this condition over the whole region due to the restriction of computer resources. Hence, the low-Reynolds-number turbulence model used in scSTREAM adopts a special boundary condition for which the strict no-slip condition is always imposed whenever the mesh size adjacent to the wall is satisfied by the condition  $y^+ \leq 1$ , while the conventional wall-function approach is applied to the region at  $y^+ \geq 11.6 = y_v^+$ . In the in-between region ( $1 \leq y^+ \leq y_v^+$ ), both boundary conditions are connected with each other via the following formulations:

$$k = \left( \frac{y^+}{y_v^+} \right)^2 \frac{u^{*2}}{\sqrt{C_\mu}} \quad y^+ \leq y_c^+$$

$$\varepsilon = \frac{2\nu k}{y^2} + \frac{y}{y_v} \left( \frac{u^{*3}}{k y_v} - \frac{2\nu k}{y_v^2} \right) \quad y^+ \leq y_c^+$$

This wall boundary condition, named hybrid wall boundary (HWB) condition, allows the low-Reynolds-number turbulence model being used for simulating wall turbulent flows with coarse meshes near the wall. For industrial type applications this helps since it is computing saving (few mesh grids are needed near the wall) but it has also some drawbacks: firstly the  $y_v^+$  is not always constant but it is strongly dependent by the flow nature; secondarily for some turbulent flow simulations this hybrid wall function is not adequate. For instance when separation and reattachment phenomena occur the damping function  $f_\mu$  become zero since the  $y^+ = \frac{u_\varepsilon y}{\nu}$  always becomes zero due to a zero friction velocity.

To overcome all this Craft *et al.*[11] developed an analytical wall-function (AWF) in a more general level than the log-law based schemes. In the AWF, the wall shear stress and heat flux are obtained through the analytical solution of simplified near-wall versions of the transport equation for the wall-parallel momentum and temperature, accounting for effect in smooth and

rough wall turbulent flow [11; 12]. In particular, rather than using a conventional damping function it has been thought to shift the turbulent origin from the wall to the edge of the viscous sublayer. Hence the turbulent viscosity is taken as zero within the viscous layer, while for  $y \geq y_v$  the same is assumed to increase linearly with the distance from the edge of sublayer:

$$\mu_t = \max\{0, \alpha \mu (y^* - y_v^*)\}$$

where  $y^* = \frac{y\sqrt{k}}{\nu}$  is the new non-dimensional distance, while  $y_v^* = \frac{y_v\sqrt{k}}{\nu}$  is the edge of the viscous sublayer. The new non-dimensional wall-normal distance is quite effective in flow with separation and reattaching points because of the non-vanishing turbulence kinetic energy  $k$  at those points.

### 3. Numerical Simulation

#### 3.1. Turbulence model validation

In this section the experimental results obtained by Meinders [2] are compared against numerical predictions. Benchmark criteria were based on the prediction of surface temperature profiles on some specified path and velocity profiles at different heights. The test channel is similar to the one proposed in [3]. Since the test layout allows a symmetry boundary condition along the central in-plane, half of the domain was considered. The whole dimensions are  $23H \times 3.4H \times 4H$  in the streamwise ( $x$ ), normal to the channel ( $y$ ) and spanwise ( $z$ ) directions, where  $H$  is the cube size ( $H = 15$  [mm] as pointed out in [2]). All the computations have been performed with an Intel Xeon E5645 2.4GHz machine (2 processors and 12 cores).

The simulation consists of two sub-domains: firstly a channel domain used as driver region (in blue color) and secondarily a wall-mounted cube domain which is inside the first one (in black color). The channel domain is solved to get the transition from laminar to turbulent boundary layer. As addressed in [3] in cases with flow separation, free shear layers, laminar-turbulent transitional flows, the downstream flow is highly dependent on the condition specified at the inlet. On the contrary of what is performed in [1], where the heat conjunction problem of heated wall-mounted cube was resolved in a single analysis domain with a turbulent flow fully developed, in the present communication the resulting flow consists of developing turbulent boundary layer both on the floor and on the opposite wall. Although this flow is qualitatively comparable to the fully developed channel one, a noticeable difference exists in local heat transfer from the cube [2]. This might be seen comparing the surface temperature profiles obtained in this study with the ones shown in [1]. Since the resulting profiles are in accordance with the experiments they are used as inlet conditions for the simulation of the wall-mounted cube by means of the so called zooming function. In scSTREAM [6], the zooming function enables to apply an analysis result to initial conditions and/or boundary conditions in another analysis. An analysis result of upstream flow field can be used for inlet boundary condition of another analysis. Moreover zooming function enables to link any field parameters of different mesh sizes. So it can link global large size analysis and local small size analysis.

*Channel domain: Turbulent characterization* Channel flow simulations were carried out using the low-Reynolds turbulent models before introduced and the resulting flow fields are used as inlet conditions for the simulation of the wall-mounted cube.

The test layout allows a symmetry boundary condition along the central in-plane, half of the domain was considered. A non-conformal mesh was used with a computational grid set of  $93 \times 115 \times 41$  points in the  $x$ ,  $y$  and  $z$  directions, respectively. A total number of 438,495 cells were used. A cluster of grid points at the walls has been used so that the  $y^+$  is often less than 1. Symmetry, wall friction and free-stream conditions were applied at the domain boundaries. The outlet zone is set as fixed static pressure at 0 [Pa]. Since the inlet velocity is 4.47 [m/s] and the

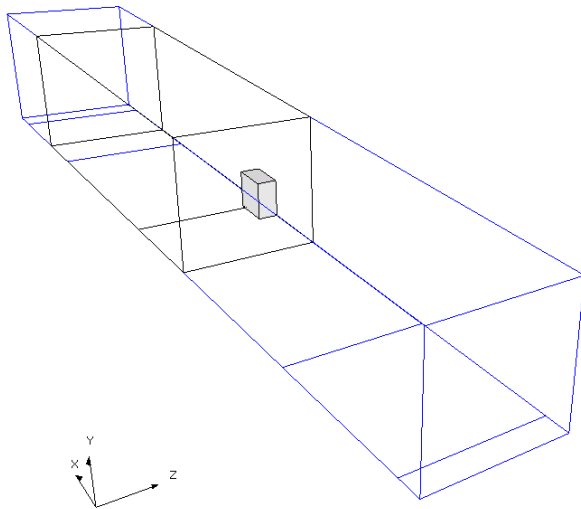


**Figure 1:** Whole computational domain

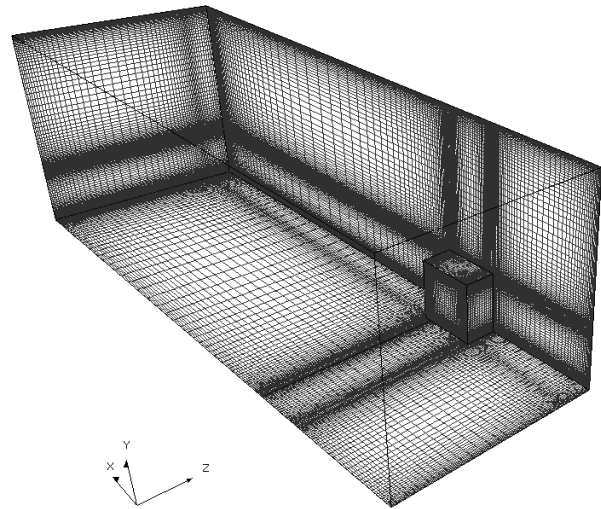


**Figure 2:** Wall-mounted cube domain mesh, 3D view

reference length is  $H$ , the Reynolds number is approximately 4440 [2]. The convergence level reached by the residual is at least  $1e-6$ .

*Wall-mounted cube domain: Validation study* Since the origin of the axis system, the inlet and the outlet of computational domain are located at  $x = -2H$  and  $x = 4H$ , respectively, while the cube is located between  $0 \leq x \leq H$ ,  $0 \leq y \leq H$ ,  $-0.5H \leq z \leq 0$ . The computational grid is set in  $154 \times 123 \times 53$  grid points in the  $x$ ,  $y$  and  $z$  directions, respectively. A non-conformal mesh was used in the streamwise and wall-normal directions with grid points clustering near the channel and cube walls. The total number of cells is about one million. In comparison with the channel case the number of grid points has been doubled in a volume which is half of the whole one. The mesh of the wall-mounted cube domain is shown in 2.

The test channel base plate is constructed by phenol-formaldehyde which is  $10 [mm]$  in thickness and has a thermal conductivity from  $0.33 [\frac{W}{mK}]$ . The structure of the cube can be decomposed into two materials: the core of the cube measuring  $12 [mm]$  is constructed from copper, with a thermal conductivity of  $398 [\frac{W}{mK}]$ , which is kept at constant temperature of  $75 [C]$ . The second material is an epoxy resin, with a thermal conductivity of  $0.24 [\frac{W}{mK}]$ , which encapsulates the copper and has an uniform thickness of  $1.5 [mm]$ . The ambient temperature was set at  $21 [C]$ . In table 1 are addressed the numerical parameters used for the simulations. The convergence level reached by the residual is at least  $1e-7$ .

**Table 1:** Numerical parameters used for the simulations. Legend: U,V,W= Mean Velocity Components, T=temperature, TQ=Turbulence Quantities,UW=upwind(1st order), QK=QUICK(2nd order)

	Spatial Discretization			Pressure Correction	Under-Relaxation			
	U,V,W	T	TQ		U,V,W	P	T	TQ
<b>linear AKN</b>	UW	QK	UW	SIMPLEC	0.9	1	0.9	0.6
<b>nonlinear AKN</b>	QK	QK	UW	SIMPLEC	0.9	1	0.9	0.2
<b>thermal AKN</b>	QK	QK	UW	SIMPLEC	0.6	1	0.9	0.6

*Comparison* Surface temperature and velocity fields are presented in Figures 3, 5 and 6. The experimental data used can be found in Meinders *et al.* [2].

In figure 3 the streamwise velocity profiles are shown at a location of  $x/H = 18.7$  downstream the inlet at the centreline of the channel (i.e. at location of  $x/H = 6.7$  far from the cube origin). It is evident that all the turbulence models match quite well the profile in the bulk flow, in the meanwhile all the models severely under-predict the wake region of the cube since they seem to still recover after the recirculation region. Similar results can be found in [13]. In figure 4 streamline plots in xy-plane and xz-plane are shown and compared with a DNS simulation and experimental visualization, respectively. It can be noted that all the features addressed in [2] are present: the horseshoe vortex at the base of front face and its saddle point, the arch vortex in the wake recirculation region and the vortex tube at the side. Among the three turbulence models presented the thermal AKN gives the best results. Indeed the locations of all the vortical patterns are in good accordance with respect to the experiment and the DNS visualizations. Analysing the velocity profiles at  $z/H=0$  in figure 3, along path upstream and downstream the cube, again one can recognise that the thermal AKN model qualitatively represents better the experimental data, in particular it is able to individuate the vortex position upstream and downstream the cube by means the minimum of its curves. The nonlinear is the farthest from the experiments. It can be said also that for all the models it is evident that the shear layer separated at the top leading edge reattaches more farther than it should do.

Temperature experimental data were collected with an Infrared Thermography (IR) technique with accuracy within 0.4 [C]. More inaccuracies might be found at the corners of the cube, due to the restriction of such a data retrieval system. The surface temperature profiles are shown in figures 5 and 6. Looking at figure 5, for the leeward face of the cube (AB) it can be said that the AKN  $k - \varepsilon$  turbulence model produces a good comparison against the experimental data, suggesting that the wake flow vortex resident in this region is accurately predicted. Also the nonlinear one shows good performances, while the thermal model over-estimates the range. Looking at the top face (BC) the linear AKN is compliant with the measured peak of the bound recirculation region while it fails to catch the thermal trend before it. The thermal AKN model behaves similarly to the linear AKN. The nonlinear over-estimates the whole range implying much more diffusion than the experiments. For the windward face (CD) since an over estimation of the turbulent kinetic energy generated near the stagnation point the numerical results under-estimate the measured values, so the thermal trend is predicted only in qualitative way by all the models.

The same comparison can be made over the in-plane path, see figure 6. For the lateral faces (AB) and (CD) linear and thermal AKN catch the peak where the recirculation happens, while the nonlinear completely over-estimates the data. For the windward face (BC) all the three models under-predict the experimental data. For the leeward face (DA) the linear AKN matches well the thermal behavior.

According to the comparison before seen and since the thermal AKN model is expensive in terms of computational time, it can be stated that the linear AKN is thought being the best choice to be used in the electronic cooling simulation over a real test case.

### 3.2. Infotainment and Navigation Systems (INS) thermal problem

To test the turbulence model chosen a real test case is taken into account. As known, 3D numerical models involve very expensive computations, both for hardware and time needed for obtaining reliable results. In [1] time was spent in analyzing hypotheses able to simplify the virtual model, maintaining the same standard of result's reliability. The simplification of physical

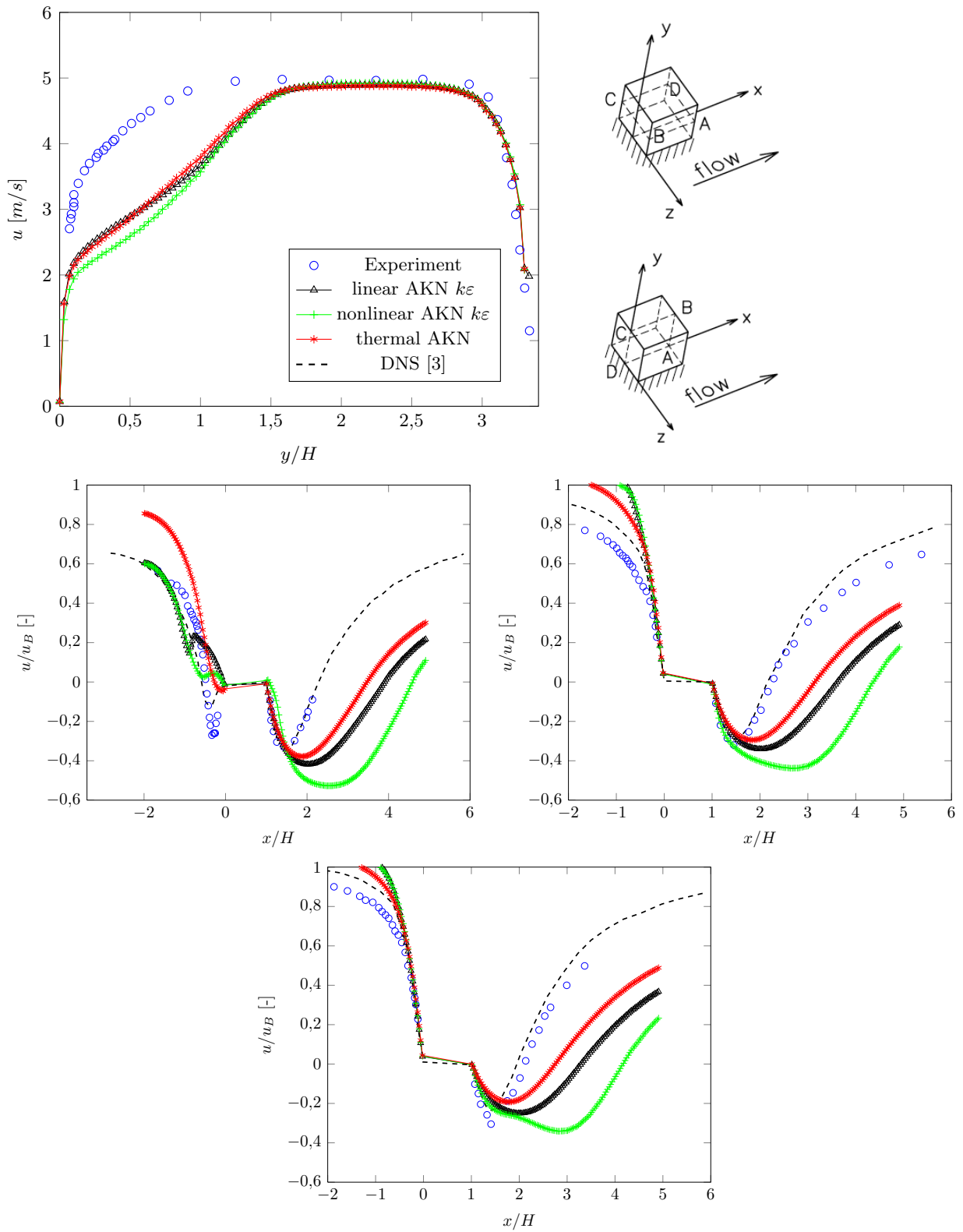


**Figure 3:** Streamwise velocity profiles at  $x/H = 18.7$  (top-left). Cube's path ABCDA and ABCD for surface temperature profiles (top-right). Dimensionless streamwise velocity profiles ( $u_B$ =bulk velocity) at  $z/H = 0$  for different heights:  $y/H = 0.1$ ,  $y/H = 0.3$  and  $y/H = 0.5$

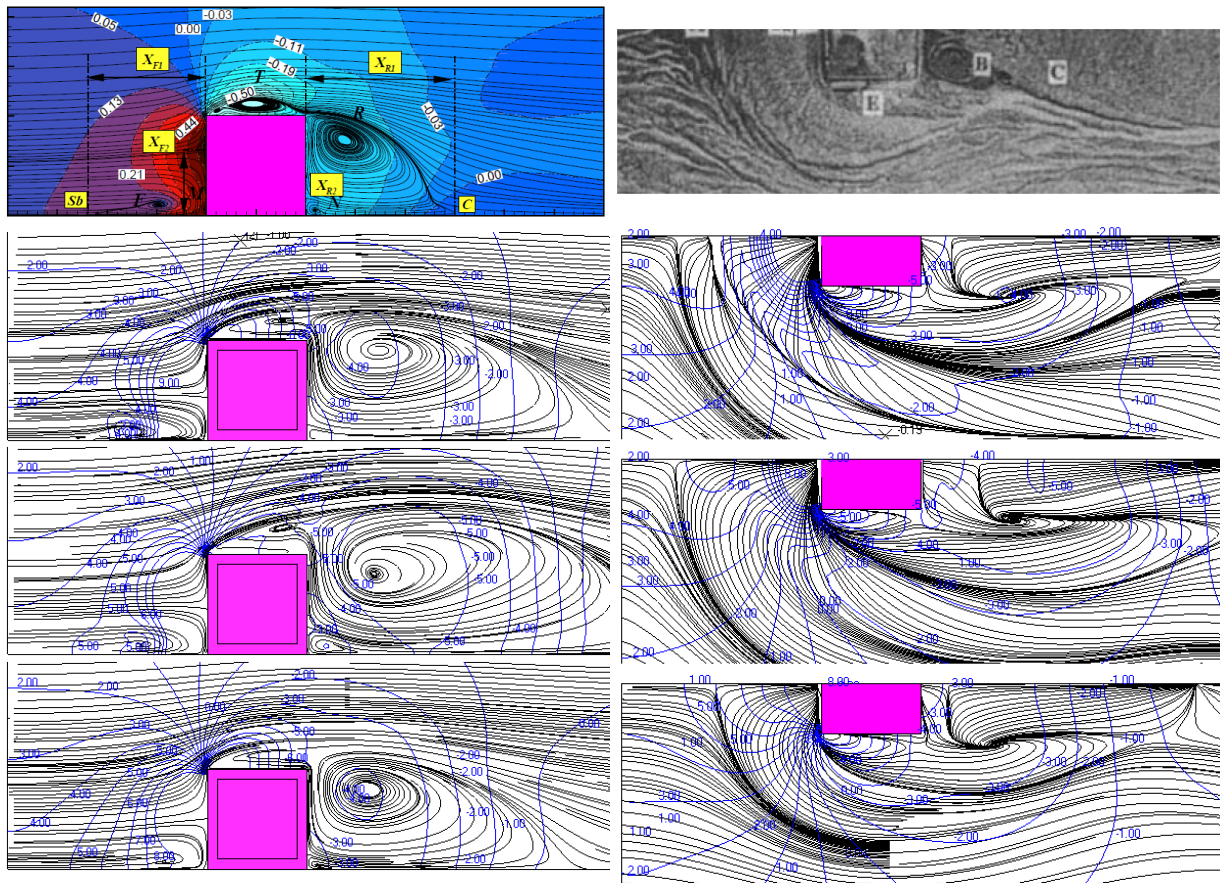


**Figure 4:** Visualizations of the surface flow and pressure distribution. from left to right and from top to bottom: DNS [3], Experiment [2], linear AKN, nonlinear AKN and Thermal AKN

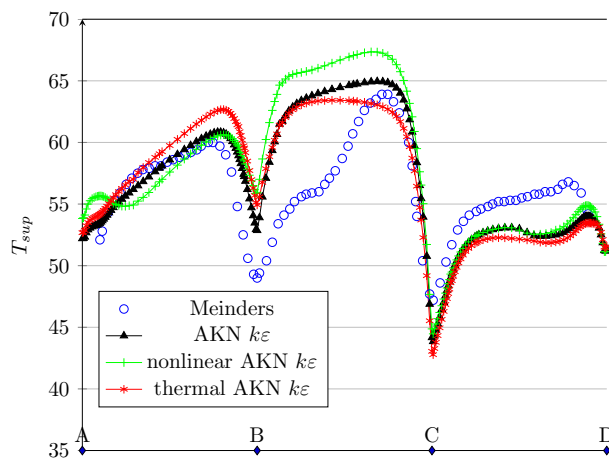


**Figure 5:** Surface temperature profile along path ABCD

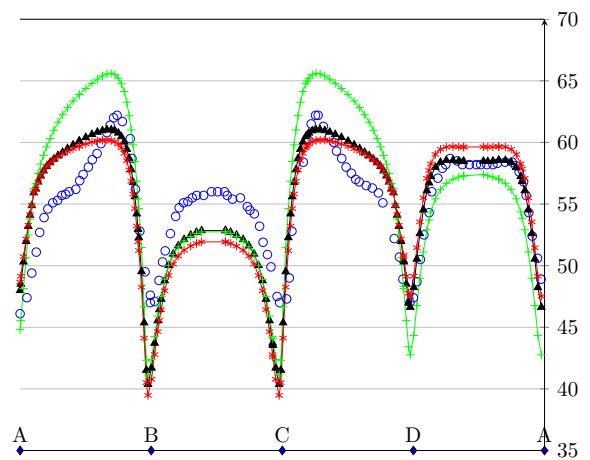


**Figure 6:** Surface temperature profile along path ABCDA

system allows drastically reducing degrees of freedom of the numerical model, so that memory space and computational time can be saved.

An infotainment and navigation system (INS) during operative conditions has been considered, see figure 7. The system mainly consists of three printed circuit boards: Main Board (MB), Daughter board (DB) and Power Board (PB). The electronics is all contained inside a metallic case, whose external dimensions are  $195 \times 165 \times 53 \text{ mm}$ . It presents several multimedia and connectivity devices such as Wi-Fi, Bluetooth, Cd-Rom etc. The electronics layout is suited to generate thermal interactions among components: it is an useful case to test very complex numerical models. The system presents an outlet fan working at  $6200 \text{ RPM}$ , with a pressure-flow rate curve from 0 to  $5.75 \text{ mmAq}$  and flow rate from 0 to  $0.28 \text{ m}^3/\text{min}$ . During the idle condition the electronic system dissipates about  $18 \text{ W}$ , while during the operative test, with a sinusoidal waveform applied, it dissipates about  $39 \text{ W}$  (efficiency of the amplifier: 18%).

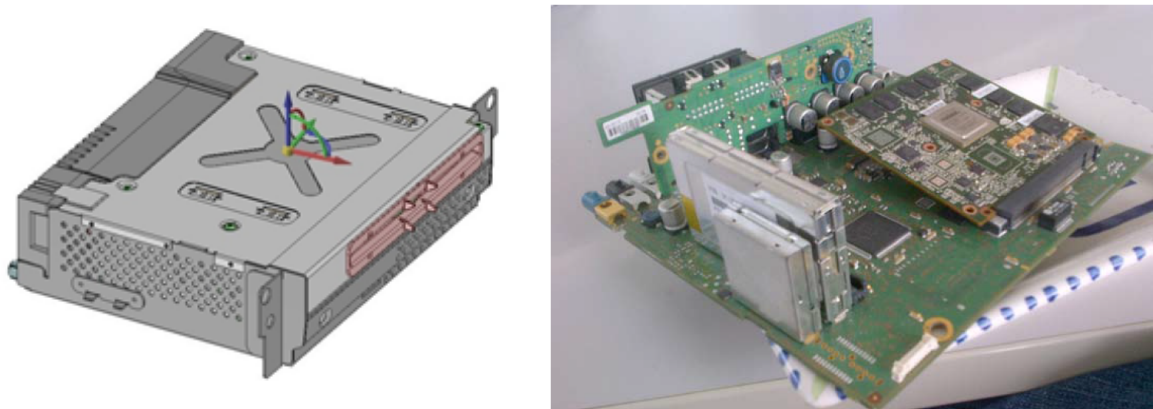


**Figure 7:** A real test case: infotainment and navigation system (INS)

Ambient temperature was set at  $65 \text{ C}$ . Since the INS was tested in a climatic chamber the boundary conditions imposed to the domain are: the friction and adiabatic wall for the bottom face, without introducing any errors the lateral faces were considered as free stream while a fixed total pressure was imposed at the top face.

Because of the absence of a characteristic length useful to describe the flow regime, the problem has been solved both in laminar and in turbulent regime. It is also reported the simulation with and without radiative heat exchange mode. Generally, when a forced ventilation is used, the radiative heat exchange might be considered negligible since the contribute in the heat exchange is minimal compared to the other two modes of heat transfer. In our case, however, the high velocity flow is confined only in a given area of the electronic device due to the design of some internal parts, so then all the remaining parts of the system also exchange in radiative way. This fact is well proven by the comparison between numerical and measured values, see table 2.

#### 4. Conclusions

This study highlights the opportunity to exploit numerical approaches in order to simulate the thermo-fluid-dynamic behaviour of complex electronic devices. The study underlines the unquestionable importance of a validation step for the numerical model, strictly needed in order to assure effectiveness and reliability of the results carried-out. The accuracy of the numerical

**Table 2:** Prediction Discrepancy: measured vs. virtual temperatures

	DDR2	Daughter PCB	Heat spreader	Heat sink	Fan outlet air	Mother PBC
<b>laminar flow + no-radiation</b>	1.77%	1.36%	3.0%	3.94%	5.74%	5.14%
<b>AKN model + radiation</b>	1.13%	1.65%	0.1%	0.1%	2.49%	1.92%

models used is assessed against experimental measurements. The detected temperature values are well in accordance with experimental data.

## References

- [1] Giannuzzi M and Selci A 2013 Thermal predictions for an infotainment and navigation systems (ins). an experimental vs. numerical correlation *Proceedings of 31th UIT Heat Transfer Conference, ISBN 97888-6493-017-6* pp 329–338
- [2] Meinders E R, Hanjalic K and Martinuzzi R J 1999 *Journal of Heat Transfer* **121** 564–573
- [3] Yakhot A, Liu H and Nikitin N 2006 *International Journal of Heat and Fluid Flow* **27** 994 – 1009 ISSN 0142-727X
- [4] Abe K, Kondoh T and Nagano Y 1994 *International Journal of Heat and Mass Transfer* **37** 139 – 151 ISSN 0017-9310
- [5] Abe K, Kondoh T and Nagano Y 1995 *International Journal of Heat and Mass Transfer* **38** 1467 – 1481 ISSN 0017-9310
- [6] Software Cradle Co., Osaka 530-0001 Japan 2011 *scSTREAM, Thermofluid Analysis System with Structured Mesh Generator*
- [7] Iaccarino G 2001 *Journal of Fluids Engineering* **123** 819 ISSN 00982202
- [8] Launder B and Sharma B 1974 *Letters in Heat and Mass Transfer* **1** 131 – 137 ISSN 0094-4548
- [9] Klebanoff P 1955 Characteristics of turbulence in a boundary layer with zero pressure gradient Tech. rep. NASA
- [10] Kays W M and Crawford M E 1993 *Convective Heat and Mass Transfer (Third Edition)* (McGraw-Hill) chap Chapter 13
- [11] Craft T, Gerasimov A, Iacovides H and Launder B 2002 *International Journal of Heat and Fluid Flow* **23** 148–160 ISSN 0142727X
- [12] Suga K, Craft T and Iacovides H 2006 *International Journal of Heat and Fluid Flow* **27** 852 – 866 ISSN 0142-727X special issue of the 6th International Symposium on Engineering Turbulence Modelling and Measurements
- [13] Dhinsa K K, Bailey C J and Pericleous K A 2004 Turbulence modelling and its impact on cfd predictions for cooling of electronic components *In Thermomechanical Phenomena in Electronic Systems -Proceedings of the Ninth Intersociety Conference*